J. Phys. D: Appl. Phys. **33** (2000) 3198–3213. Printed in the UK PII: S0022-3727(00)14903-4

Removal of cyclohexanone in transition electric discharges at atmospheric pressure

Zdenko Machala†‡, Marcela Morvová†, Emmanuel Marode‡ and Imrich Morva†

† Institute of Physics, Faculty of Mathematics and Physics, Comenius University, Mlynská Dolina F2, 842 48 Bratislava, Slovakia
‡ Laboratoire de Physique des Gaz et des Plasmas, EDEE, University Paris-Sud XI, Supelec, Plateau de Moulon, 91 192 Gif sur Yvette cedex, France

E-mail: machala@fmph.uniba.sk, morvova@fmph.uniba.sk, marode@lpd.supelec.fr and morva@fmph.uniba.sk

Received 22 June 2000

Abstract. Two new types of streamer-induced electric discharges operating in a non-uniform electric field in air at atmospheric pressure were applied to the removal of volatile organic compounds (VOCs). The first type is a pulseless dc discharge with physical properties corresponding to the glow discharge. The second, also supplied by a dc high voltage of both polarities, is a spontaneously pulsing discharge operating in the regime of the streamer-to-spark transition, the spark phase being too short to reach local thermodynamic equilibrium conditions. Both discharges are able to generate a non-thermal plasma, as resolved from their rotational and vibrational temperatures.

The influences of these discharges on the removal of cyclohexanone at various gas flow rates and concentrations (600–6000 ppm) were compared. The removal efficiencies achieved were about 50–60%, and the energy costs were 16–100 eV/molecule at various energy densities. Special conditions where CO_2 and other gaseous products are minor and dominant products appear in the condensed phase can be obtained, especially in the spontaneously pulsing transition discharge.

We explain some plasmochemical processes induced by the discharges by considering heterogeneous effects of the copper electrode surface. The role of active nitrogen and the formation of the NCO radical are probably key factors leading to the formation of the condensation product based on amino acids, here produced for the first time from VOCs, as well as in the overall energy cycle resulting in low energy costs of the process.

The small pilot-scale reactor based on the spontaneously pulsing transition discharge has been successfully applied to the removal of cyclohexanone in the mixture with other VOCs with no noxious gas output. This validates the possibility of the application of such a type of reactor for larger scales.

1. Introduction

Many recent papers deal with the removal of various aliphatic and mainly aromatic hydrocarbons. The most frequent non-thermal plasma techniques used for VOC decomposition are electron beams, dc and pulsed coronas, dielectric barrier discharges, ferroelectric packed bed reactors etc, sometimes combined with catalysts [1–15]. The initial parameters, such as the treated VOC and its input concentration, residence time in the reactor, etc, vary widely. Thus, results of the decomposition process achieved in these techniques are also rather dispersed. The basic parameters characterizing this process that allow us to compare the various techniques are the removal efficiencies, energy costs and products formed.

In most of the non-thermal plasma processes the energy generated by the plasma is directed preferentially to electron impact dissociation and the ionization of the background gas molecules. Produced reactive radicals decompose the targeted pollutants (electron beam, pulsed corona techniques and some dielectric barrier discharge techniques). In contrast, a high-temperature plasma is used in thermal plasma furnaces or torches where the entire gas is heated and thermal decomposition occurs.

Recently, non-thermal plasma techniques using discharges with medium temperatures (1000–2000 K) give good results in the decomposition of VOCs and other gaseous pollutants (for example, some dielectric barrier discharge reactors [13] and gliding arcs [16]). In such plasmas it is probable that both of the above phenomena participate at the removal of pollutants. The thermal decomposition occurs close to the discharge channel. At the same time, the energetical electrons, ions and excited species induce the dissociations and creation of radicals which enter into the decomposition reactions.

0022-3727/00/243198+16$30.00

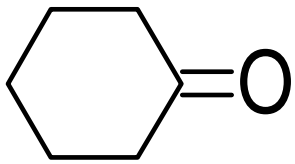

Structure 1. Cyclohexanone.

In order to apply the simultaneous effects of a relatively high discharge temperature and non-equilibrium conditions to the VOC decomposition we present two new types of electric discharges: a high-pressure pulseless glow discharge and a spontaneously pulsing streamer-to-spark transition discharge, they will be described in more details in the following. Their application to the removal of cyclohexanone and a comparison of their properties and chemical effects are focussed on this paper. The new plasma technique for VOC removal uses additional effects of a heterogeneous catalysis on the copper electrode surfaces. The role of the light emitted from the discharge is probably also important.

The rotational T_r and vibrational T_v temperatures of a discharge can be determined from its emission spectra [17]. They give valuable information on the temperature of the gas in the discharge and on the type of the plasma. The rotational temperature, T_r, tends to equilibrate with the kinetic temperature of heavy species at high pressures, i.e. with the gas temperature. If the plasma is in local thermodynamic equilibrium (LTE) T_r should be equal to T_v, if this condition is not fulfilled the plasma is non-thermal (non-equilibrium).

There are only just a few publications on the removal of VOC using electric discharges similar to those which are presented in this paper. A pulseless atmospheric-pressure glow discharge in the capillary reactor was used for the dissociation of methane [18] and a dc glow discharge at atmospheric pressure in a multipoint reactor was applied to the removal of toluene [19]. These two discharges are similar to the high-pressure glow discharge presented here. A pulsed discharge operated in a capillary tube reactor, which is electrically similar to the spontaneously pulsing transition discharge presented here, was used for the destruction of various VOCs (toluene, TCE, etc) [20].

Cyclohexanone ($C_6H_{10}O$) is a six-membered cyclic ketone with the chemical structure shown in structure 1.

Under normal conditions it is a colourless, volatile, unpleasant smelling liquid, with a saturated vapour pressure of 600 Pa at 25 °C and a boiling point of 156.7 °C. We used cyclohexanone as a VOC representative for three reasons. First, it is widely used in industry, For example for the production of adipic acid, polyamides 6 and 6.6, the amino acid lysine, as a solvent for various materials (such as cellulose and its acetates and nitrates, PVC, paints, waxes, fats and lubricants) and for the production of glues for PVC, etc [21]. Second, it is toxic to living organisms; vapours of cyclohexanone cause eye, throat and nose irritation, in higher concentrations it attacks human skin and liver. Third, due to its cyclic non-aromatic structure its behaviour in electric discharges differs from the aromatic (e.g. toluene, benzene) and the aliphatic (e.g. formaldehyde, acetates, alcohols, aliphatic ketones) VOCs which are usually tested in plasma treatment.

Except our preliminary study [22], the treatment of cyclohexanone in plasma applications of VOC removal has not been published, The only reported similar cyclic non-aromatic VOCs treated by plasmas are cyclohexene and cyclohexane. Futamura *et al* [23] reported the destruction of cyclohexene in a ferroelectric packed bed reactor with efficiencies of up to 80–90%, increasing with specific energy density (cyclohexanone has been present among the by-products in wet N_2). Bailey *et al* [24] used a dc corona discharge to decompose up to 80% of the cyclohexene and other VOCs present. Up to 80–90% of the cyclohexane present in a mixture with other hydrocarbons extracted from petrol was removed in a dc corona combined dielectric barrier discharge, as reported by Jaworek *et al* [5].

For other ketones, the 45–80% decomposition of aliphatic methyl-ethyl-ketone (MEK) in a silent discharge plasma was reported by Chang and Chang [11]. They formed the usual gaseous products, such as CO_2, CO, HCOH, NO_x and some solid products.

Most of authors using plasma techniques as environmental applications tend to decompose VOCs into non-toxic gaseous CO_2 and H_2O. However, this VOC removal process is usually accompanied by CO and NO_x production and some products in the condensed phase or aerosol often appear in the reactor. Furthermore, environmental applications producing CO_2 are also not ideal, because CO_2 is a main contributor to the increasing greenhouse effect on the Earth. In our experiments the aim is to convert VOCs into non-toxic, preferentially, solid products and to decrease the CO_2 production. Minimal production of other toxic gases (CO, NO_x etc) has to be controlled at the same time.

Morvová *et al* [25, 26] and Hanic *et al* [27] found the formation of amino acids in the dc corona discharge in the N_2–CO_2–H_2O systems with Cu electrodes. The experiments were primarily aimed at CO_2 depletion, but similar mechanisms can also occur in the N_2–VOC and N_2–CO_2–H_2O–VOC systems. This process passes via the formation of long-lived NCO, OC–NCO and ON–NCO radicals which lead to the formation of amino acids, amides and some heterocyclic chemical structures (pyrrol ring, oxamidate complexes of Cu, etc). Copper electrodes influence these processes heterogeneously. An advantage of such processes is that they do not produce CO_2, but non-toxic products in the solid or liquid phases. Similar solid products have been found in our experiments with a high-pressure glow discharge applied to the removal of aromatic VOC [28].

The most important new approach of the VOC removal plasma technique presented in this paper is that toxic VOCs are converted into non-toxic condensed products based on amino acids, with almost no production of other toxic and greenhouse gases.

2. Experimental details

2.1. Electrical discharges used

Two kinds of electrical discharges were tested for the destruction of cyclohexanone. They have been named

according to their properties: 'high-pressure glow discharge' and 'spontaneously pulsing (streamer-to-spark) transition discharge' (or 'transient spark'). The abbreviations 'HPGD' and 'SPTD' will be used in the following. Both types of discharge are maintained by a dc high voltage of both polarities applied onto the metal electrodes of a corona geometry forming a non-homogeneous electric field.

The external circuits of both discharges used contain an external resistance R which has a stabilizing and protection function. R is in the range of 100 kΩ–1 MΩ for HPGD and 2–5 MΩ for SPTD. In the case of SPTD the capacity C of the order of 10s of picoFarads has to be present in the discharge part of the circuit, behind the external resistance R. Usually, C is represented by an internal capacity of the discharge chamber $C = C_{int}$ (discharge tubes used for cyclohexanone destruction); if C_{int} is too low, an external capacitor parallel to the discharge has to be added, then $C = C_{ext} + C_{int}$ (point-to-plane discharge chamber used for emission spectroscopy). The capacity C is responsible for the pulses in SPTD, it is unessential for pulseless HPGD, figure 1.

Some physical properties such as vibrational and rotational temperatures of both kinds of discharge used have been measured by means of emission spectroscopy. The experimental set-up used for these measurements was composed of a special discharge chamber with a point-to-plane electrode configuration linked with the emission spectroscopy system containing a monochromator, Jobin Yvon HR640; control system, OMA; photomultiplier, Hamamatsu C 659 S; 400 MHz digital oscilloscope, Tektronix DSA 602; and a PC (described in more detail in [29]). A technique of the comparison of the experimental and simulated emission spectra of the second positive system of N_2 corresponding to the $C^3\Pi_u$–$B^3\Pi_g$ electronic transition was used for rotational temperature determination (bands of 0–1 and 1–2 transitions, with an accuracy about 20 K). Several bands of the same N_2 system were taken to determine the vibrational temperatures (accuracy 100 K).

2.2. Discharge chambers and electrical parameters of the discharges used in the VOC destruction process

The experiments aimed at VOC removal in the HPGD were carried out in a rectangular transparent discharge chamber ($2 \times 3.5 \times 80\,cm^3$). The chamber comprises a copper rod with a thread (diameter 6 mm) as a high-voltage electrode opposite two copper planes as low-voltage grounded electrodes with an interelectrode distance of 7 mm. In fact, the threaded rod represents many points. Gas flow rates of $Q > 6\ l\ min^{-1}$ enable the discharge channel to move along the stressed electrode (from one point to another). The value of the external resistance of $R = 300$ kΩ was used in order to lower the energy losses and to assure the stable pulseless regime.

We used a cylindrical discharge chamber with the high-voltage threaded rod electrode (as above) for the tests on the influence of the SPTD on cyclohexanone, figure 1. Both the rod and the cylinder were made of copper, the inner diameter of the cylinder was 21 mm, the interelectrode distance was 7.5 mm and the length of the discharge tube was 50 cm. The internal capacity of this discharge chamber

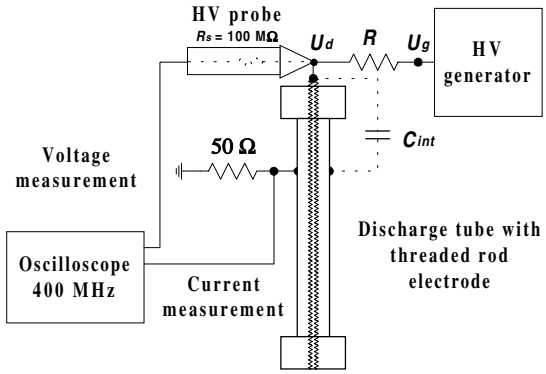

Figure 1. Discharge tube with threaded rod—experimental set-up for electric measurements.

was approximately 30 pF. $R = 5$ MΩ was used to avoid the transition into the HPGD regime. The discharge migrated along the rod even without gas flow; with gas flow its migration is enhanced.

The electrical parameters of the discharges, such as discharge current and voltage, were measured in each experiment. The discharge current and voltage were detected by a 400 MHz digital oscilloscope, Tektronix DSA 602 using a high-voltage probe, Tektronix T 6015A (3 pF, 100 MΩ), and a 50 Ω resistance (for current measurements). The mean current and potential of the generator U_g were measured by dc meters.

The typical discharge current and voltage in the HPGD of both polarities were about $I = 5$ mA at $U = 1.6$–2 kV. The generator voltage U_g is evidently higher:

$$U_g = U + RI.$$

In the SPTD, the mean values of the current and generator voltage were about $I = 2$–2.5 mA and $U_g = 14$ kV (negative polarity) or $U_g = 16$ kV (positive polarity).

The total power spent in the whole system was calculated from the generator voltage and the total mean current for both discharges:

$$P = U_g I.$$

Thus, the energy losses in the external resistance are included in P.

2.3. Gas flow system and VOC concentration

Experiments aimed at the destruction cyclohexanone were carried out in the flowing regime, figure 2. Dry air from a pressure tank was used as a carrying gas. The air flux was divided into two branches controlled by two flowmeters with different ranges, one branch passes through the bubbler with liquid VOC. The adjustment of the flowmeters enables one to change the VOC concentration in the gas. The total gas flow value can also be varied.

The concentration of cyclohexanone was calculated from its saturated vapour pressure (0.6 kPa at 25 °C) with verification of the absorbance of certain calibrated bands in the infrared (IR) spectra. This makes the maximal concentration approximately 6000 ppm at room temperature (25 °C).

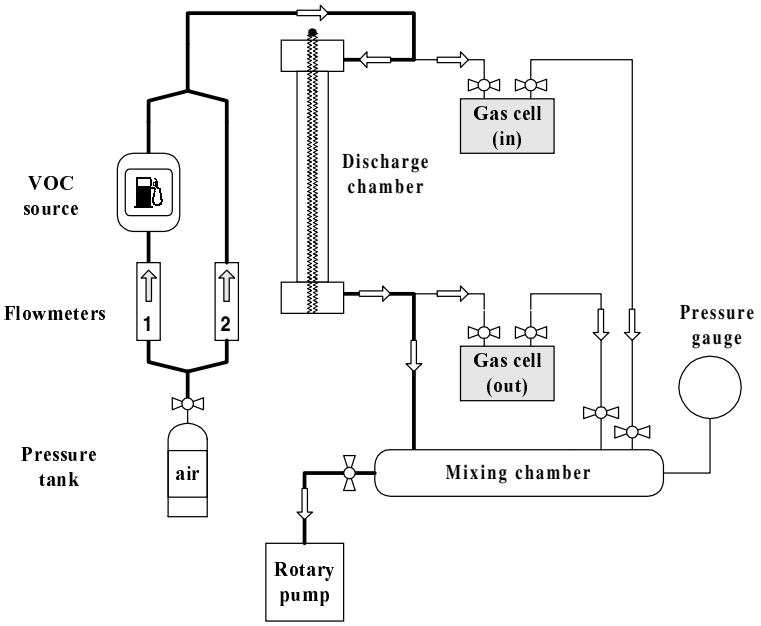

Figure 2. Gas flow system adapted for isokinetic sample acquisition.

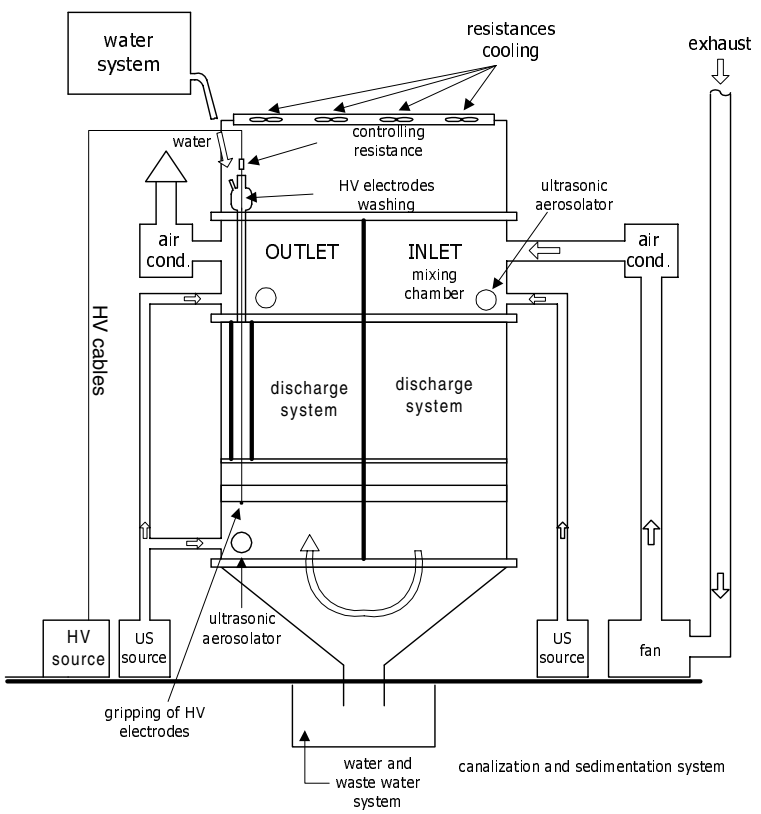

Figure 3. Schematic diagram of the small pilot-scale discharge reactor.

An isokinetic acquisition of samples was applied, i.e. the gas cells collecting samples in front of and behind the discharge chamber were on two bypasses, linked to the main flow system, including the discharge chamber. The gas flow through the bypasses was many times lower than in the main system, therefore the closing of the gas cell valves did not affect the flow parameters of the main system. The whole system was pumped by the rotary pump in order to control the atmospheric pressure everywhere.

2.4. Small pilot-scale discharge reactor

The effects of the SPTD on cyclohexanone were verified in the small pilot-scale discharge reactor, figure 3. These

tests were performed on the bypass of the exhaust system on a production floor where cyclohexanone was used. The exhaust was composed of air at ambient temperature enriched by the vapours of cyclohexanone and some other VOCs (ethyl acetate, ethyl benzene, toluene, xylene) and exhaust of natural gas combustion.

The discharge reactor consists of two main sectors with 12 parallel 50 cm long coaxial discharge tubes in each one. The inner electrodes are threaded by cooper rods (6 mm diameter), the outer electrodes are brass cylindrical tubes with 18 mm inner diameter. These discharge tubes are very similar to those used in the laboratory measurements. The two sectors form the U-shape of the reactor, the first one leads the gas down and the second one up. The whole device was equipped with two fans (one before and one after the reactor), two gas flowmeters posed similarly and hermetically closable holes for various probes.

A dc high voltage of both polarities was applied to all discharge tubes from the high-voltage power supply giving up to 20 kV at a maximum power 500 W with a 50 Hz transformation frequency. Each electrode was equipped by its own series resistance in the range 1.8–5.8 MΩ. The total discharge current (sum of the currents in each discharge tube) and voltage were measured by dc meters.

2.5. Diagnostics

The IR absorption spectroscopy was used as the main diagnostic method. The spectra were obtained by a dispersive spectrometer, SPECORD M 80, working in the middle and far-infrared regions (4000–200 cm^{-1}). The chemical changes in the gas phase were determined from the comparison of the samples before and after discharge action. The solid products deposited on the surfaces of the discharge chamber were determined either directly on the surfaces by the technique of reflection spectroscopy, or collected and analysed in KBr pellets.

Additional techniques, such as gas chromatography, were used for the analysis of the gaseous products of the bypass measurements. Solid products were also analysed, by x-ray diffraction, thermogravimetry and high-precision liquid chromatography (HPLC).

3. Results and discussion

3.1. Properties and mechanisms of the electric discharges used.

The HPGD is pulseless, the oscilloscopic waveforms of its voltage U and current I are flat lines, with fluctuations caused by noise. The HPGD is initiated by a streamer developing into a spark, but the current I does not fall to zero after the spark pulse, it rests at certain value in the order of 1 mA. A new streamer cannot develop after this, because the discharge potential is too weak (1.6–3 kV for an interelectrode gap of 7 mm). No more pulses appear and the discharge remains pulseless. It is stable due to the condition of equilibrium between ionization and electron attachment.

The HPGD in air is characterized by a luminous violet channel and by the fact that it does not make any noise. The current on voltage dependence (I–V characteristics) of the discharge is negative. The HPGD was studied in more detail in our paper [29], a larger study is also being prepared for publication. It was called a 'high-pressure glow discharge' because its properties and mechanisms are very similar to the glow discharge known at low pressures. Typical regions of the glow discharge can be distinguished in both polarities of the HPGD, such as the cathode layer, the negative glow, the Faraday dark space and the positive column.

Positive and negative HPGDs have very similar properties (electric parameters, light intensity profiles, temperatures). The polarity of the high voltage applied on the point electrode is important only for discharge ignition. As soon as the stable discharge is established, it becomes less important, the discharge behaves approximately in the same way whether the point electrode is a cathode or an anode, i.e. the cathode region forms close to the cathode (point in HPGD− and plane in HPGD+), etc.

The SPTD is a filamentary discharge of a streamer-to-spark transition type. The mechanism of its function is similar to the prevented spark developed by Marode *et al* [30]. It is initiated by a streamer which transforms into the spark pulse formed due to the discharging capacity C (represented usually by an internal capacity of the discharge tube). The spark cannot develop into an arc because C is too low, the energy stored in it is not sufficient for spark development. Once C is discharged, which occurs very quickly, the high spark current I falls to zero due to the voltage fall on the external resistance R. This discharge does not have properties of a typical spark discharge (LTE), the spark phase is too short. This is why we also named it the 'transient spark'. During the quenched phase, with no conductive current, the discharge capacity C is recharged by the growing potential on the stressed electrode. Usually, during this relaxation phase there also appears a corona discharge in its glow regime and some pre-streamers. As soon as C is again charged enough, it feeds a new transient spark pulse. This process repeats with a frequency of several kilohertz, which is not absolutely regular, and causes the characteristic noise of the discharge. The frequency increases with increasing applied voltage.

The name 'spontaneously pulsing transition discharge' was used for several reasons. The discharge has a pulsed character, although the applied voltage is dc. The pulses are not controlled just by the external circuit of the discharge, but also by the internal properties of the discharge tube, especially its internal capacity, which probably changes as deposit layers are formed on the electrodes. The process of pulse formation is spontaneous in a certain way, it depends on the parameters of electric circuit, as well as on the time of operation and involved plasmochemistry. Furthermore, the name SPTD comprises the transient spark phase of the discharge and the relaxation phase with corona discharge and pre-streamers.

Typical oscilloscopic waveforms of the discharge potential and current of the SPTD are presented in figure 4. An initiating streamer ($t = 300$ ns) and its transition to the transient spark ($t = 380$ ns) is visible on the $I(t)$ dependence. The discharge voltage drops dramatically as the current increases. The streamer-to-spark phase of the process is three orders of magnitudes shorter than the post-spark relaxation phase.

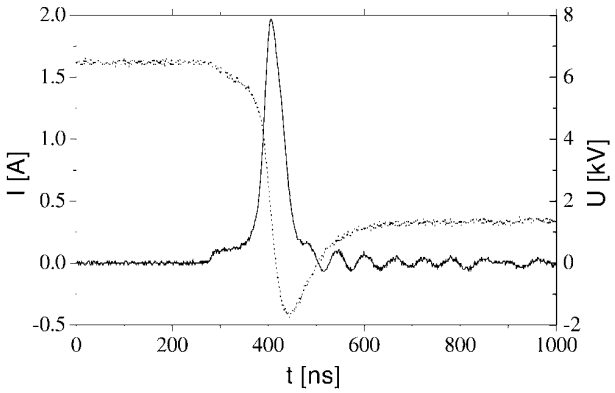

Figure 4. SPTD in a positive point-to-plane configuration: gap 7 mm; voltage, U(kV) (· · · · · ·), and current, I (A) (——) waveforms for $U_g = 9.3$ kV, $I_{average} = 0.73$ mA, and $R = 5$ MΩ.

Visual observation of the discharge gives the impression of a brush composed of the strongly shining white–blue channels. A human eye, capable of 0.1 s resolution of visual images, can see several hundred transient sparks at the same moment, because the pulse frequency is in the order of kilohertz.

3.2. Discharge temperatures—generated plasma

The determination of the rotational T_r and apparent vibrational T_v temperatures of the discharges was performed. The method of evaluating the apparent vibrational temperature is to measure the distribution of intensity of the second positive nitrogen band heads, and to infer the vibrational temperature of the ground state by using Frank–Condon factors (which govern the upper vibrational states distribution when they are produced by electron impact from the ground state) [31]. Actually, the obtained figures of T_v are only indicative as we will discuss it in the next section, while the rotational temperature T_r can be more surely taken as the local gas temperature T_g. The temperature determination gave the following results.

- HPGD. T_r = 1400–2300 K, T_v = 3500–4500 K, T_r increases and T_v decreases with increasing discharge current; for I = 5 mA T_r = 2200–2300 K and T_v = 3500–3600 K.
- SPTD. T_r = 500–1700 K (increases from anode to cathode), $T_v \sim 8000$ K (for $I = 0.95$ mA).

In spite of such high temperatures the discharge plasmas of both discharges is out of LTE since $T_r \neq T_v$. The regime of HPGD is closer to LTE than the SPTD regime.

3.3. Discussion about the validity of these temperatures

Let us first discuss the question of the various temperatures of the neutral N_2 molecules under the condition of the discharges studied.

The duration of the SPTD lies in the tens of nanoseconds range (maximum of 100 ns). The created plasma can hardly reach LTE conditions in this short time. The SPTD works with a frequency ranging between 1–10 kHz, which corresponds to 0.1–1 ms of the relaxation time without the current. On the other hand, the HPGD burns continuously, with a temperature of about 2000 K in the channel. This explains why the plasma formed in the HPGD is more thermal than in the SPTD, this feature will be shown even later from the point of view of the plasmochemistry. Actually, the SPTD is preceded, some hundred nanoseconds before, by a preconditioned situation established by a streamer discharge. Under such a condition, Tholl [32] shows that the transient plasma temperature may reach several tens of thousands of degrees. Let us analyse more precisely our case.

The streamer begins to produce a plasma bridge between the cathode and the anode due to the crossing of a streamer ionization wave. The plasma bridge is a cold cylindrical plasma, whose neutral temperature T_g remains at about 350–400 K. The electrons running through this plasma filament have, however, an electron temperature well above the neutral one. Their mean energy reaches 1–2 eV, i.e. 7000–15 000 K (on the basis of a temperature conversion given by $3/2kT_e$) [33]. Due to this high mean electron energy, the electrons ionize and excite the molecules and, namely, excite various levels of rotations and vibrations. The large value of the electron energy is due to the small electron energy loss during elastic collisions. The electron energy is mainly consumed by inelastic collisions. Moreover, in the case of air 90% of their energy goes towards vibrational excitations, increasing drastically the vibrational temperature of N_2 [34]. Indeed, the number of collision undergone by each electron with neutrals at atmospheric pressure is in the order of 3×10^3 collisions over 10 ns (on the basis of a mean collision cross section in the order of 1×10^{-15} cm^{-2} and 2 eV). Without collisions between heavy species, the distribution of rotation and vibration levels of the molecules inside the cold plasma column would thus reflect the electron energy distribution, rather than the neutral temperature distribution. Before the transient spark appears, at least some hundreds of nanoseconds before, this cold plasma channel prepares the gas inside the path of the transient spark.

The question now is: how will this stored energy in the rotational and vibrational levels react with collisions between heavy species? Since the energies between rotation levels are of the same order of magnitude as the energy corresponding to the neutral speed, a quick relaxation of the rotational energy towards a thermal equilibrium with the neutral species will happen. Thus the rotational temperature of the ground state should quickly relax to T_g, and the intensity distribution of the rotational components into a molecular band may be used to derive T_r [31].

This is, however, not the case with the level of vibrations. Since the energy between two consecutive vibration levels (for low values of v) are much larger than the thermal energy, the vibrational to translation collisions (i.e. vibration to translation transfer) are very small and rather the vibration to vibration dominates. It has been shown that such a situation, where a group of molecules excited vibrationally share their energy through a vibration to vibration transition (with $\Delta v = +1$ or -1), leads to a vibration distribution of the Treanor type [35]. This distribution is somewhat different from the Boltzmann distribution for high v levels, but is near a Boltzmann distribution for small v levels. In pure nitrogen, the relaxation of vibrational levels at atmospheric pressure

Table 1. Selected results of the cyclohexanone decomposition in dry air at various gas flows and concentrations in HPGDs and SPTDs, with positive and negative discharge polarities.

Discharge and polarity	P (W)	Q (l min^{-1})	τ (s)	c_0 (ppm)	η (%)	R_v (J l^{-1})	R_m (kWh kg^{-1})	R_{mol} eV/molecule
HPGD+	21.5	2	12.10	2350	77	643.6	24.6	89.5
	16.5	6	4.03	1450	66	165.0	11.9	43.4
	16.5	8	3.02	1650	46	123.8	11.3	41.0
	15.1	18	1.34	1600	34	50.3	6.4	23.2
HPGD−	16.5	2	12.10	2150	83	495.0	19.2	69.8
	17.0	6	4.03	4150	66	170.0	4.3	15.6
	16.5	8	3.02	1950	61	123.8	7.2	26.2
	22.8	12	2.02	1150	52	114.0	13.2	48.0
	17.5	18	1.34	1200	43	58.3	7.8	28.4
SPTD+	40.8	3	3.18	2100	45	815	59.7	217.4
	41.0	6	1.59	2800	58	410	17.6	64.1
	39.4	10	0.95	2850	44	236.2	13.1	47.7
	42.0	18	0.53	1900	42	140	12.1	43.9
SPTD−	31.2	3	3.18	1950	53	624.8	42.2	153.5
	34.0	6	1.59	1700	69	340	20.0	73.5
	31.7	10.1	0.94	2600	62	188.2	8.0	29.3
	31.7	18	0.53	2700	37	105.6	7.3	26.4

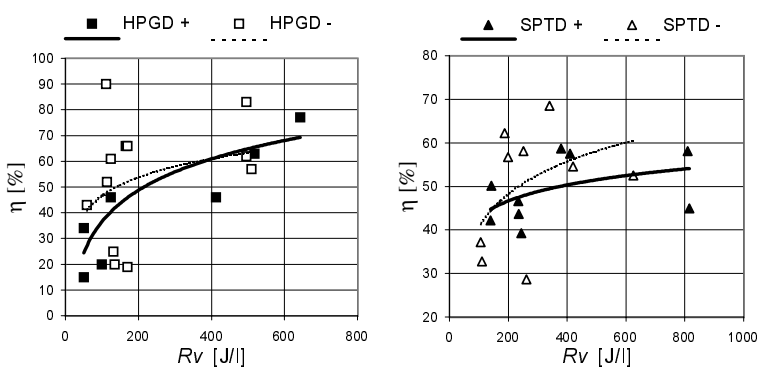

Figure 5. Chemical efficiency as a function of the energy density R_V, for both polarities of HPGD and the SPTD.

requires some hundreds of microseconds. In the presence of oxygen this figure should change only a little (it is mainly in the presence of CO_2, used as pump of $N_2(v)$ in the CO_2 laser, that the vibrations of N_2 are quickly destroyed, which is not the case here). The existence of the filamentary cold plasma several hundreds of nanoseconds before the transient spark is thus largely insufficient to allow a relaxation of the vibrational distribution towards T_g, and thus T_v (determined from low values of v) may be much larger just before the transient spark arises. At high pressure, within the filamentary 'pre-transient spark' state, the rotational temperature T_r should be near T_g while the vibrational temperature T_v should be between T_g and T_e.

Now, when the electrons excite a population of nitrogen molecules with its specific vibrational distribution towards the C states, it will reflect somehow the distribution of the ground state. Only somehow, since the excitation will follow the various values of the Frank–Condon factors (which are $v = 0$ to $v' = 0/0.54$, 0 to 1/0.3, 0 to 2/0.107, 1 to 0/0.347, 0 to 2/0.267, 0 to 3/0.18, 0 to 4/0.08, the transitions not listed being negligible) [36]. Due to these non-uniform Frank–Condon factors the upper distribution in the C state of the vibration level does not have the same shape as the ground state. If the upper-state vibrational distribution is not perturbed by heavy species collisions, it is possible to infer the initial ground-state vibrational distribution i.e. T_v. However at atmospheric pressure, the collisions between heavy species are numerous, and quenching of the upper $C\,^3\Pi_u$ state happens. Do these collisions drastically change the distribution of the vibrational states not destroyed by the quenching? The question raises three remarks.

First, following the studies on C state extinction by the quenching effect [37], it is mainly due to O_2 collisions. The pressure quenching for the $v' = 0$ and the $v' = 1$ of the C state are, respectively $p_0 = 3.57$ Torr and $p_1 = 2.67$ Torr. While depletion of the $v' = 1$ state should be more important, it however does not change drastically the upper v' distribution.

Second, the derivation of T_v from the upper state assumes implicitly, that these upper states are due to the collisions of electrons with the ground state. This assumption is probably not completely correct, since a non-negligible fraction of the upper-state production may come from the A or B nitrogen states.

Finally, the fact that N_2 (C, $v' \neq 0$) state may end at N_2 (C, $v' = 0$) due to collisions with N_2 (X), thus overpopulating the $v' = 0$ state [37] may change the distribution of the v' states; but this last effect can only lead to a lowering of the value of the apparent T_v.

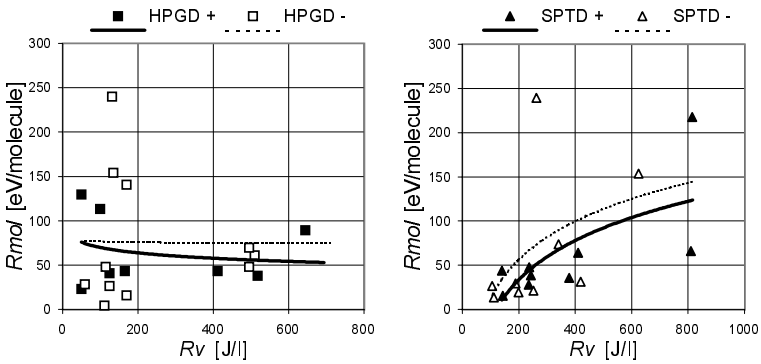

Figure 6. Energy costs R_{mol} as a function of the energy density R_V, for both polarities of the HPGD and the SPTD.

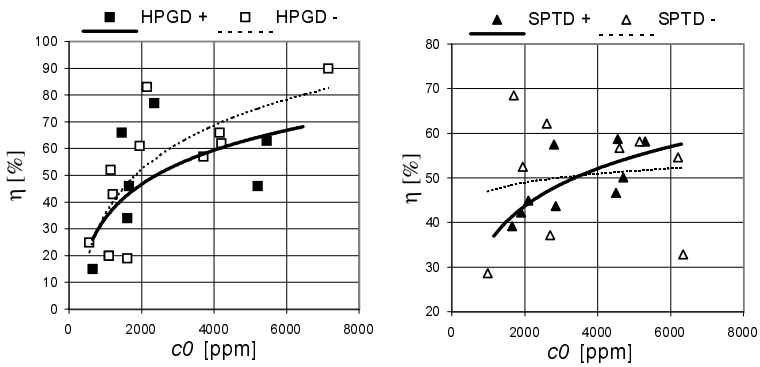

Figure 7. Chemical efficiency η as a function of the initial concentration c_0, for both polarities of the HPGD and the SPTD.

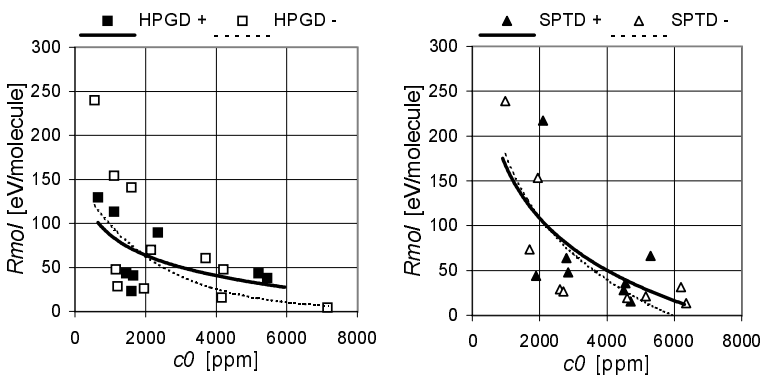

Figure 8. Energy costs R_{mol} as a function of the initial concentration c_0, for both polarities of the HPGD and the SPTD.

In conclusion, while the value of 8000 K given for T_v in the SPTD case should be taken as an 'apparent' vibrational temperature, the real T_v (at least for the distribution in the first v levels) should not be too far from this order of magnitude. Moreover, the main objective of these spectroscopic measurements, being aimed towards revealing the non-equilibrium plasma states within the SPTD and the HPGD, may be considered as fulfilled.

3.4. Results of the cyclohexanone decomposition process

Table 1 shows selected results of the experiments aimed at cyclohexanone removal in dry air at various gas flows and concentrations. The electrical discharges used were the HPGD and the SPTD of positive and negative discharge polarity. Table 1 gives the values of the total expended power $P = U_g I$, the total gas flow rate Q, the residence time in the discharge chamber τ, the input concentration of cyclohexanone c_0, (the removal efficiency $\eta = 1 - c/c_0$ (expressed in percent) where c is an output concentration of cyclohexanone), and the following energy costs:

- energy dissipated in the volume (specific energy density) $R_V = P/Q$ [J l^{-1}], it does not give any information on the destruction process;
- energy expended per kilogram of the removed compound $R_m = P/Q\eta c_0 = R_V/\eta c_0$ [kW h kg^{-1}], c_0 expressed in density units (e.g. g m^{-3}),
- energy expended per one removed VOC molecule $R_{mol} = R_m M_m/N_A$ [eV/molecule], where M_m is a molar mass and N_A is the Avogadro constant.

The energy costs are calculated with regard to the total expended power P, which includes the energy losses in the

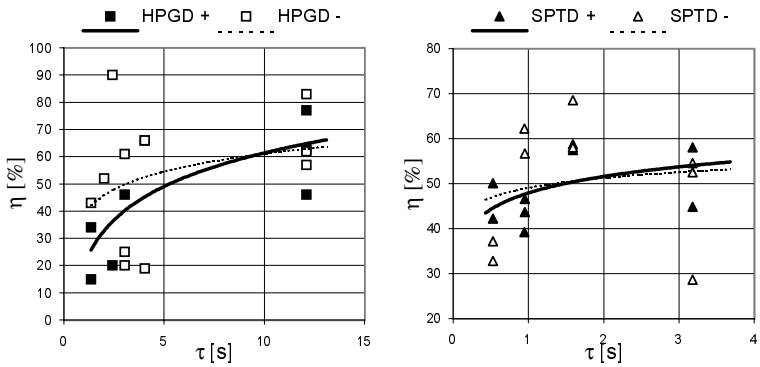

Figure 9. Chemical efficiency η as a function of the residence time τ, for both polarities of the HPGD and the SPTD.

external resistances. R_m, respectively R_{mol}, are probably the best variables characterizing the removal process, because they comprise the absolute removal efficiency η and the spent energy.

The efficiency η of cyclohexanone removal has been calculated from the decrease of the bands ν_{as} and ν_s CH_2 at 2930 and 2860 cm^{-1} and ν C=O at 1740 cm^{-1}, the most intense bands in the IR spectra of cyclohexanone, additionally checked by the γ CH_2 band at 1224 cm^{-1} and the band of the skeletal vibration of cyclohexanone cycle ν_{cycle} at 1125 cm^{-1}, figure 11.

Values of the total gas flow Q and input concentration c_0 were changed regularly in the measurements, the variations of c_0 were also caused by the fluctuations of the room temperature and the changing amount of cyclohexanone in the bubbler. The total power P was kept at approximately the same value for each discharge type. The SPTD requires higher applied voltages (U_g = 14–16 kV) while the average current was 2–2.5 mA; in the HPGD we worked with a current of around 5 mA and U_g = 3–4 kV.

Figures 5–10 show the dependences of the removal efficiency η and energy costs R_{mol} on the specific energy density R_V, the input cyclohexanone concentration c_0 and the residence time τ in both discharges and polarities.

The values obtained for the decomposition rate of cyclohexanone η and energy costs R_{mol} are rather dispersed; η varied by around 50% in the positive HPGD, 60% in the negative HPGD and around 50% in both polarities of the SPTD. Logarithmic interpolation curves were used in figures 5–10 as they seemed to fit best the dispersed measured values of η and R_{mol}.

Figure 5 shows the removal efficiency η as a function of the energy density R_V. For all four cases (both polarities of the HPGD and the SPTD) η grows with R_V, as observable from the curves. To obtain higher η we have to increase R_V. However, doubling R_V does not double η, we observe a saturation effect, the energy is used less effectively. This is in accordance with the result of others [5, 8, 13, 23]. The highest η was obtained in the negative HPGD (70%), the lowest in the positive SPTD (55%).

Figure 6 shows the energy cost R_{mol} as a function of the energy density R_V. In both polarities of the HPGD, the $R_{mol}(R_V)$ dependence gives an approximately constant function. A result is that the energy costs in the HPGD are, almost, not influenced by the energy density, hence we can choose the regime with the highest η. This trend is different in both polarities of the SPTD where R_{mol} grows with increasing R_V. Thus, to decrease R_{mol} it is better to work at low R_V. For $R_V < 200$ J l^{-1} the energy costs R_{mol} are lower in the SPTD (10–50 eV/molecule, better in positive SPTD) than in HPGD (50–100 eV/molecule). For an R_V of around 300 J l^{-1} SPTD and HPGD are similar from the point of view of R_{mol}. For $R_V > 400$ J l^{-1} the removal process is more energetically effective (lower R_{mol}) in the HPGD (50–100 eV/molecule) than in SPTD (100–150 eV/molecule). The positive polarity of both discharges always give lower R_{mol}. However, the effect of the discharge polarity is rather weak, especially in the HPGD, this will also be obvious in figures 7–10. This result was expected since the properties of positive and negative HPGDs are very similar.

Figure 7 shows η as a function of the initial cyclohexanone concentration c_0. Figure 7 shows that η is affected by c_0, its trend is increasing, and is stronger for negative HPGDs. Figure 7 also shows says that the HPGD is a more convenient method to use for higher initial VOC concentrations. The values are too dispersed in the SPTD to bring any conclusions.

R_{mol} decreases with increasing c_0 (see figure 8), which is logical from the formula by which it is calculated, and shows that the strongest decrease is in the negative SPTD. Most of the R_{mol} values are in the interval 10–100 eV/molecule, such energy costs are rather low. Here we can see a problem point when the removal process is characterized only by energy costs—it might seem excellent if the input concentration is high, although in reality it is poor. It is better to characterize the process by more parameters (η, R_V, R_{mol}).

Finally, figures 9 and 10 show η and R_{mol} as functions of the residence time τ of the treated gas in the discharge chamber. τ is inversionally proportional to the total gas flow Q. For all discharges η increases with growing τ, for $\tau > 4$ s a saturation effect of η occurs. Hence, it is not convenient to work at low gas flows. When $\tau < 4$ s is higher in the SPTD than in HPGD, therefore the SPTD is a more convenient method for low residence times (high gas flows). The $R_{mol}(\tau)$ dependence demonstrates that R_{mol} is almost independent of τ in the HPGD, while in SPTD R_{mol} grows with increasing τ. The lowest R_{mol} was obtained in the SPTD for very low τ(<1 s). Such a regime is energetically cheap, but η is relatively low (30–50%). Putting more discharge tubes in series could improve this fact, this was a case in the pilot-scale reactor.

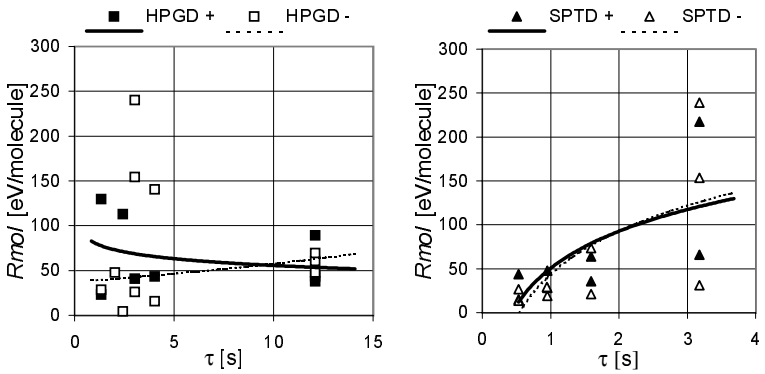

Figure 10. Energy costs R_{mol} as a function of the residence time τ, for both polarities of the HPGD and the SPTD.

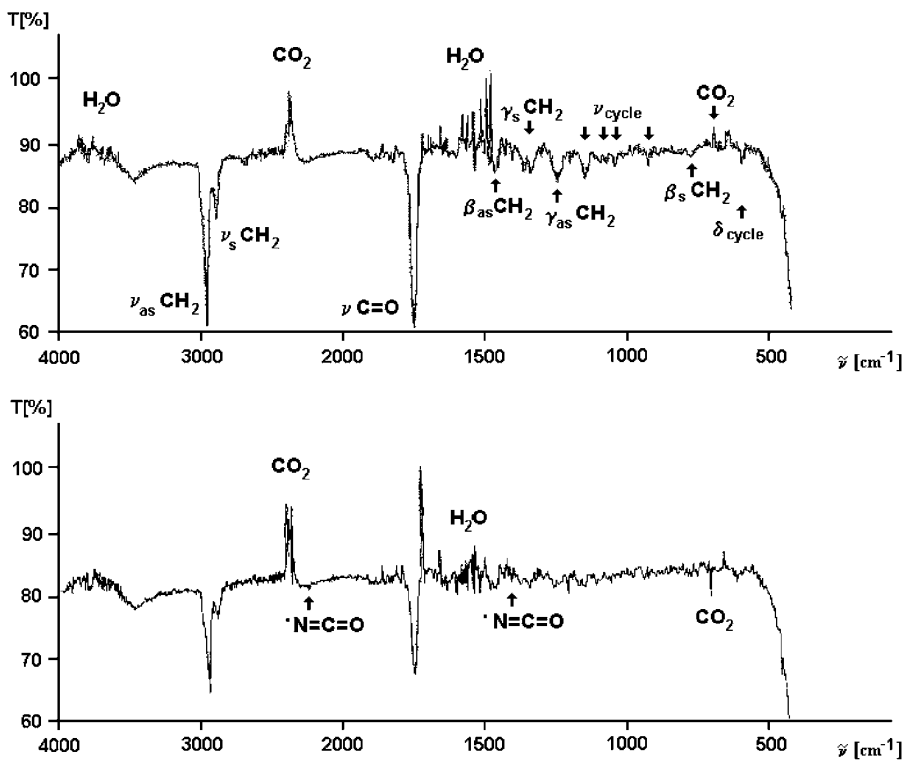

Figure 11. IR gas phase spectrum of air with cyclohexanone before (top) and after (bottom) negative SPTD ($Q = 6\,\mathrm{l\,min^{-1}}$, $c_0 = 5150$ ppm).

The removal efficiencies achieved in cyclohexanone removal by the HPGD and the SPTD might seem rather high on realizing that both these discharges are strongly constricted and occupy a small part of the discharge chamber. We suggest the following explanation of this phenomenon. VOCs are treated in the reactor in three ways which cooperate and lead to their removal:

(1) thermal decomposition occurring close to the discharge channel due to a high temperature—a minor part of the passing gas is treated directly in this way;
(2) volume reactions induced by radicals formed by the discharges occur further away and in cooler parts of the reactor—most of the passing gas is treated in this way;
(3) surface reactions on the copper electrodes—a significant amount of the passing gas is in contact with electrodes due to the hydrodynamic turbulence in the reactor (surface reactions will be explained in more detail later).

Furthermore, the discharges, especially the SPTD, move quickly in the discharge tube axially (along the discharge tube) and radially (around the stressed electrode). These motions enhance the contanct of the passing gas with the discharge and increase the turbulence, which results in a more effective VOC treatment.

3.5. Products and involved plasmochemistry

Vapours of cyclohexanone in dry air were converted into some gaseous and some solid (condensed) products. Their character depends on the type of the discharge, the residence time τ of the gas in the discharge volume and the initial cyclohexanone concentration c_0. The discharge polarity,

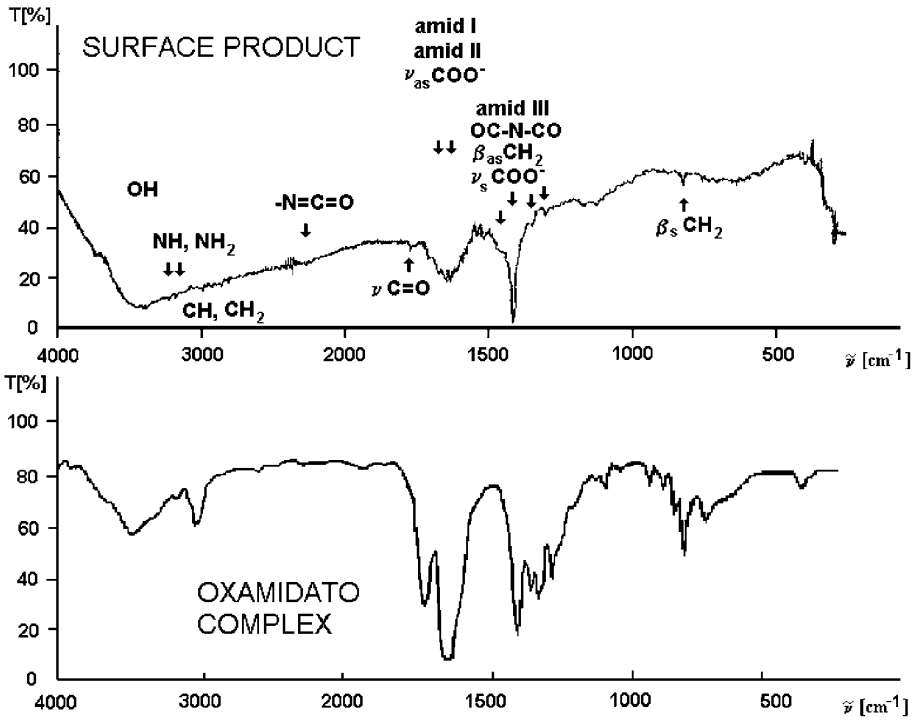

Figure 12. IR spectrum of the solid product formed on Cu electrode surfaces after cyclohexanone decomposition in both polarities of the SPTD (top) compared with the spectrum of oxamidato complex from [40] (bottom).

although having an influence the discharge properties, has an effect on the products formed.

In the HPGD of both polarities and very long residence times (12 s) we detected a strong CO_2 and H_2O production (about 4000 ppm) with some CO production (maximum 100 ppm), similar to most of the plasma VOC removal applications. H_2O production was stronger in the negative polarity. NO_2 was formed in maximal concentrations of 200 ppm. Other gaseous species such as NO, O_3 were not detected. Such a process is similar to the thermal combustion of cyclohexanone.

With decreasing τ, in the HPGD the CO_2 and H_2O production decreased; on the other hand, new products appeared. NO_2 might have been present in a low concentration (below 50 ppm).

CO_2 (240 ppm), CO (160 ppm), NO_2 (maximum 80 ppm) and H_2O were produced in the positive polarity of an SPTD with long τ (3 s). Their creation was very weak (100–120 ppm CO_2 and 24 ppm CO—limit of detection) at short τ (0.5–1 s). The situation was similar in the negative SPTD, CO_2 (300–560 ppm), CO (100 ppm), NO_2 (maximum 40 ppm) and H_2O were produced at long τ and only 40–200 ppm of CO_2, traces of CO and some H_2O were produced at short τ. The creation of condensed products was dominant in the SPTD, especially at short τ.

Typical IR spectra of air with cyclohexanone before and after negative SPTD treatment are shown in figure 11. Important bands are marked. All IR spectra for other discharges, polarities and various parameters have been precisely analysed, but are not shown here.

The new band at 1370–1390 cm^{-1} always appeared in the gas product IR spectra, in positive polarity this is usually shifted to 1360 cm^{-1} and in negative polarity this is shifted to 1400 cm^{-1}. This band was also present in especially strong intensity in the spectrum of the solid product formed on the discharge electrodes (figure 12). In the gas phase this band corresponds to the long-lived NCO radical (formed from CO_2 after incorporation of electronically excited molecular nitrogen N_2^* $A\,^3\Sigma_u^+$) and related ON–NCO and OC–NCO intermediates. This spectroscopic band in the condensed phase is composed of the –N–CO groups present in amides (amide III band), imide group CO–N–CO, deformation of β_s CH_2 and the ν_s COO^-. The next strong and broad band, at 1680–1580 cm^{-1}, in the solid product spectrum corresponds to amide I and amide II and ν_{as} COO^-. Other bands of medium and weak intensity in the solid product belong to stretching and deformation vibrations of CH_2, NH, NH_2 and OH groups. All of these groups indicate the presence of amino acids in the product.

The IR spectra of the gas phase and solid products allow us to view some of the decomposition mechanisms of cyclohexanone and probable reaction pathways occurring in the discharge chamber.

In both discharges and both polarities the decomposition process of the cyclohexanone begins with the opening of its ring. When the residence time of the gas in the discharge is long, oxidation reactions prevail and the process is similar to combustion (forming CO_2, H_2O, CO and NO_2). This has been observed in particular in the HPGD at long τ (=12 s).

Active molecular nitrogen N_2^* (in its long-lived metastable state $A\,^3\Sigma_u^+$ with an energy of 6.17 eV [39], and probably vibrationally excited to 6.75 eV [27]) is a key species in governing the decomposition process at shorter residence times, especially in the SPTD. This active molecular nitrogen has an impact on the cyclohexanone cycle,

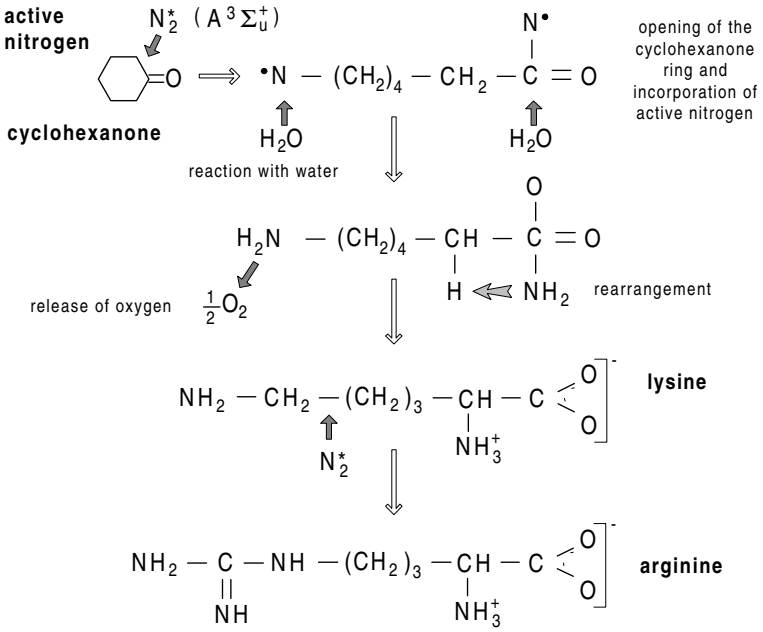

Scheme 1. Suggested formation of amino acids lysine and arginine from cyclohexanone supported by the active N_2 species.

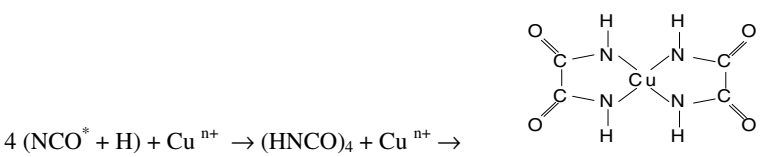

Scheme 2. [27]. NCO radical leading to the formation of an oxamidato complex on the Cu electrode surface.

which results in the cyclohexanone opening and the products being incorporated into the hydrocarbon residues.

Amino acids of C_6 type were detected in the solid product formed on the electrode surfaces. Cyclohexanone leads, in particular, to lysine NH_2–$(CH_2)_4$–$CHNH_2$–COOH which can be further converted to arginine NH_2–CNH–NH–$(CH_2)_3$–$CHNH_2$–COOH. We suggest the reaction scheme of scheme 1.

Activated N_2^* can also be incorporated into the CO_2 or CO formed in the oxidation process to create a long-living NCO radical, and ON–NCO and similar intermediates. These species are involved in the formation of electrode surface catalytic processes. An important part of this process is connected with the formation of oxamidato complexes on the Cu electrode surface, as shown in reaction scheme 2.

Hydrogen, necessary for the above reaction, is probably produced in the process of CH_2– group dehydrogenation during the lysine to histidine conversion occurring in the near electrode area. We suggest the scheme illustrated in scheme 3.

The amino acid histidine $C_3N_2H_3$–CH_2–$CHNH_2$–COOH is formed directly on the Cu electrode surface, the surface reutilizes released H_2 to form the oxamidato complex. The IR spectrum of the surface product is very similar to the spectrum of the oxamidato complex (figure 12), identified amino acid components are superposed on the bands of the complex. The high dielectric constant of the oxamidato complexes is responsible for their catalytic properties; the previously described formation of other amino acids is enhanced by these surface properties, although an exact mechanism is not known.

The introduction of water into the discharge volume leads to the preferential production of carboxylic acids, especially adipic acid COOH–$(CH_2)_4$–COOH, due to the larger concentration of OH radicals. The presence of the adipic acid in the product was confirmed from IR spectra (see scheme 4).

The processes of the incorporation of the active species of N_2^* (or N^*) and the formation of amino acids require a certain amount of energy (to produce nitrogen excites states). It is possible that the energy of radiation (UV and visible) emitted from the discharge is used, as well as the kinetic energy of the electrons created in the discharge via inelastic collisions with N_2 molecules. On the other hand, when the active nitrogen species are incorporated into more stable structures, some energy is released (these processes are exothermic) and can re-enter the reactions. This is a rough principle of the energy recycling in the systems studied and helps to explain why the VOC decomposition rates (η and R_{mol}) do not decreasing adequately with the decrease of the energy density (R_V) and why we have achieved such low energy costs (from 16 eV/molecule), see figures 5 and 6.

However, an exact thermochemical approach is needed to explain the energy recycling in detail. A more detailed description of the exact role of heterogeneous affect of the Cu electrode surfaces is a task for future work, although some explication was provided by Hanic *et al* [27].

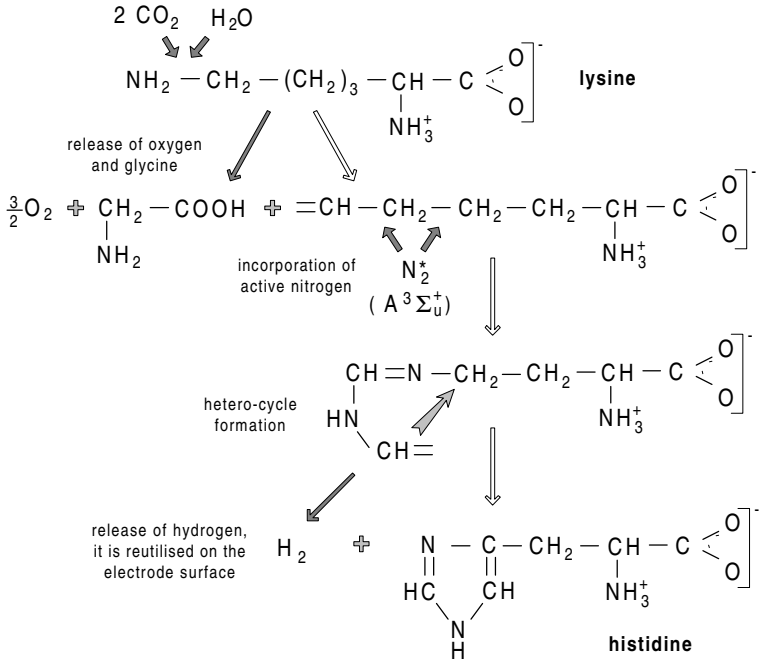

Scheme 3. Conversion of lysine to histidine on the Cu electrode surface with the help of the active N_2.

Table 2. Results of the VOC removal in the small pilot-scale reactor. VOC concentrations in mg m^{-3} and the values of energy costs are calculated with regard to the total carbon.

	Polarity					
	Positive			Negative		
VOC	c_0 (C) (mg m^{-3})	c_0 (ppm)	η (%)	c_0 (C) (mg m^{-3})	c_0 (ppm)	η (%)
Cyclohexanone	27.4	9.3	52.5	70.8	24.0	56.9
Ethyl acetate	5.2	2.6	48.6	24.7	12.6	34.2
Ethyl benzene	1.4	0.4	50.8	5.7	1.4	31.4
Toluene	0	0.0	—	1.4	0.4	100.0
Xylene	3.2	0.8	62.3	14.7	3.7	34.8
Total carbon	37.2	—	54.5	117.3	—	48.1
P (W)		133			120	
Q (l min^{-1})		580			830	
τ (s)		0.28			0.2	
R_v (J l^{-1})		14			9	
R_m (kWh kg^{-1})		189			43	
R_{mol} (eV/molecule)		686			155	

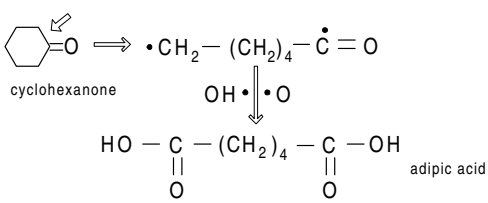

Scheme 4. Formation of adipic acid from cyclohexanone initiated by O and OH radicals.

3.6. Results of the tests in the small pilot-scale discharge reactor

The effects of the SPTD on the cyclohexanone in a mixture with some other VOCs (ethyl acetate, ethyl benzene, toluene, xylene) and products of natural gas combustion (with traces of sulfur-containing mercaptanes) were verified in the small pilot-scale discharge reactor. The initial VOC concentrations were rather low compared to the laboratory measurements. The results are drawn together in table 2. The VOC concentrations in mg m^{-3} and values of the energy costs are calculated with regard to the total carbon, hydrogen and oxygen are not taken into account.

The removal efficiencies obtained were similar to those found in the SPTD in the laboratory discharge chambers, R_v were extremely small due to high Q. The energy costs of $R_{mol} = 155$ eV/molecule (negative polarity) are acceptable, in the positive polarity R_{mol} was high due to a very low VOC concentration.

The solid product formed in the discharge reactor is a grey powder of a fractal structure on microscopic level, figure 13. It is insoluble in water and partially soluble in

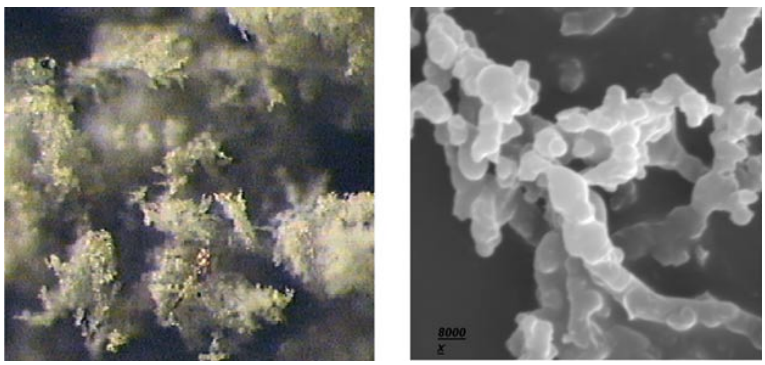

Figure 13. Micrographs of the solid product formed in the small pilot-scale reactor. Left, optical micrograph at magnification of 500×; right, scanning electron micrograph at a magnification of 8000×.

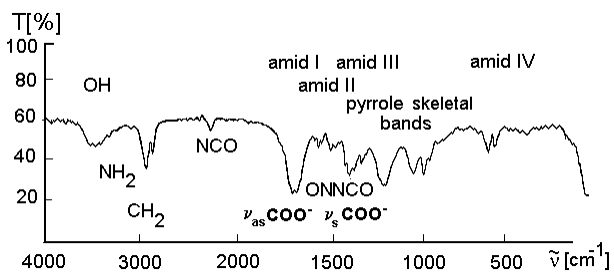

Figure 14. IR spectrum of the solid product formed in the small pilot-scale reactor.

the usual organic solvents (isopropanol, acetone, toluene, benzene). An IR spectrum of the product (figure 14) and HPLC chromatograph (figure 15) are shown. The HPLC analysis confirmed the presence of the same types of amino acids as were identified in the laboratory cyclohexanone decomposition, namely arginine, histidine and methionine ($CH_3S–CH_2–CH–NH_2–COOH$), the latter was not detected in laboratory tests, the S comes from the mercaptanes. IR analysis showed, in additions a presence of alanine, glycine, serine, lysine and aspartic acid. The main component of the powder (95–99%) is a solid condensate of amino acids and the remainder (1–5%) is an organometallic compound containing a pyrrole ring with some catalytic properties, it is formed from the Cu–oxamidato complex by the mechanisms described in [27]. Gaseous products of the process, such as CO_2, H_2O, CO and NO_x, were in negligible concentrations.

The plasmochemistry initiated by the SPTD in such a gas system is very complicated, but it is based on active nitrogen incorporation and the formation of amino acids, similar to the air and cyclohexanone mixture.

The results of the tests of the small pilot-scale reactor for VOC removal confirmed the possibility of applying the SPTD to the treatment of large volumes of gases polluted by VOCs. The process is energetically cheap and relatively effective, even at high gas flows through the reactor. The most important result is that the product of this process is a non-toxic polymer in the solid phase.

4. Conclusions

We investigated new types of non-thermal plasmas generated by the HPGD and the SPTD, and their application to the VOC removal. To conclude the important results

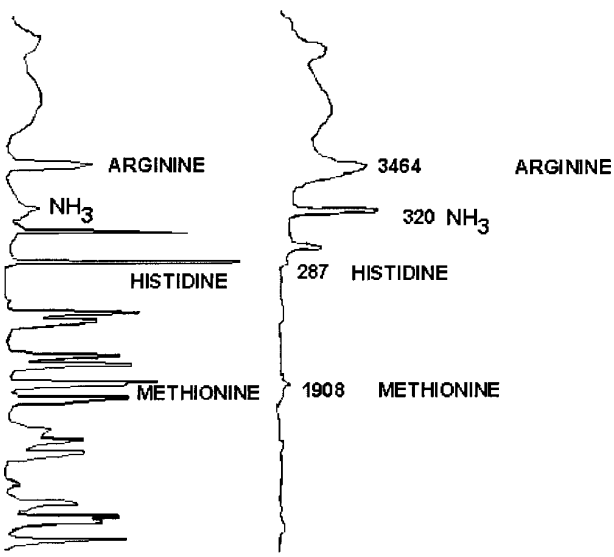

Figure 15. HPLC chromatograph of the solid product formed in the small pilot-scale reactor compared with some amino acid standards. (a) Standards. (b) Actual record of investigated system.

of the laboratory measurements in comparing the effects of these two discharges on the decomposition process of cyclohexanone, we can state the following.

- the HPGD and the SPTD are comparable from the point of view of the chemical efficiency of cyclohexanone removal. Discharge polarity does not significantly influence the efficiency.
- The energy costs are lower in the SPTD than in the HPGD, especially when the process operates at low residence times (high gas flows). The SPTD is cheaper from the point of view of energy cost. The influence of the polarity on the energy costs is weak.
- Working with higher initial cyclohexanone concentrations is always more convenient; the energy costs are lower in all cases. A similar result was achieved in [9], but contrary results were obtained in [12, 14].

In both discharges and both polarities we obtained 50–60% of a decomposition rate at energy costs of 16–100 eV/molecule and various energy densities (50–800 J l^{-1}). These energy costs are lower if compared with some other non-thermal plasma techniques [8, 11, 13]. This implies that the presented non-thermal plasmas generated in the new

transition types of discharges (pulseless HPGD and pulsed SPTD) are effective for VOC removal and are able to compete with other non-thermal plasma applications for pollution control. If all the energy losses (in the external circuit, heating of the gas and electrodes and energy irradiated as light) were subtracted, the real energy costs necessary for the cyclohexanone decomposition process would be even lower. A possible explanation of such low energy costs might be a recycling of the energy in the plasmochemical processes based on the incorporation of activated nitrogen species into CO_2 and hydrocarbon residues. Excited species of nitrogen probably work as energy reservoirs.

When the energy density of the involved discharge was high (operating at low gas flows and with long residence times in the discharge volume), the process led to the dominant formation of combustion products (CO_2, H_2O, CO and NO_2), especially in the more thermal HPGD. The same behaviour of plasmas was observed in [12, 13]. On the other hand, solid products based on amino acids were preferentially formed when the energy density was lower (shorter residence times), especially in the SPTD. Amino acids and other condensed-phase products (amides, imides) created in the tested discharges are non-toxic and more convenient from the point of view of the global Earth environment than gaseous combustion products, mainly CO_2.

HPGD and SPTD used for pollution control are neither typical non-thermal plasma applications, nor fully thermal plasma processes, but something in between. The thermal decomposition as well as the radical induced volume reactions and heterogeneous surface reactions participate in the VOC removal.

The possibility of the application of the SPTD to the VOC removal was tested in a small pilot-scale reactor. Cyclohexanone in a mixture with some other VOC was successfully removed with an efficiency of about 50–60% at a very low energy density (9–14 J l^{-1}). The process was energetically cheap and relatively effective even at high gas flows through the reactor. The major product was a non-toxic amorphous condensate based on amino acids. The tests confirmed the practical use of this method and the possibility of its application on larger scales.

Acknowledgments

The work was performed within the combined PhD studies of the first author in Slovakia and France. We thank the Slovak and French governments for providing the scholarships for these studies.

References

[1] Paur H-R 1993 Removal of volatile hydrocarbons from industrial off-gas *Non-Thermal Plasma Techniques for Pollution Control (Nato ASI Series, Part B)* ed B M Penetrante and S E Schultheis (Berlin: Springer) pp 77–89

[2] Penetrante B M, Hsiao M C, Bardsley J N, Merritt B T, Vogtlin G E, Wallman P H, Kuthi A, Burkhart C P and Bayless J R 1995 *Phys. Lett.* A **209** 69–77

[3] Penetrante B M, Hsiao M C, Bardsley J N, Merritt B T, Vogtlin G E, Kuthi A, Burkhart C P and Bayless J R 1997 *Plasma Sources Sci. Technol.* **6** 251–9

[4] Morvová M, Morva I and Kurdel M 1993 *Contrib. Plasma Phys.* **4** 285–95

[5] Jaworek A, Krupa A and Czech T 1996 *J. Phys. D: Appl. Phys.* **29** 2439–46

[6] Korzekwa R A, Grothaus M G, Hutcherson R K, Roush R A and Brown R 1998 *Rev. Sci. Instrum.* **69** 1886–92

[7] Yamamoto T, Lawless P A, Owen M K, Ensor D S and Boss C 1993 Decomposition of VOC by a packed-bed reactor and pulsed corona plasma reactor *Non-Thermal Plasma Techniques for Pollution Control (Nato ASI series, Part B)* ed B M Penetrante and S E Schultheis (Berlin: Springer) pp 223–37

[8] Smulders E H W M, van Heesch B E J M and van Paasen S S V B 1998 *IEEE Trans. Plasma Sci.* **26** 1476–84

[9] Neely W C, Newhouse E I, Clothiaux E J and Gross C A 1993 Decomposition of complex molecules using silent discharge plasma processing *Non-Thermal Plasma Techniques for Pollution Control (Nato ASI Series, Part B)* ed B M Penetrante and S E Schultheis (Berlin: Springer) pp 309–20

[10] Chang J S 1993 Energetic electron induced plasma processes for reduction of acid and greenhouse gases in combustion flue gas *Non-Thermal Plasma Techniques for Pollution Control (NATO ASI Series, Part A)* ed B M Penetrante and S E Schultheis (Berlin: Springer) pp 1–32

[11] Chang M B and Chang C C 1997 *AIChE J.* **43** 1325–30

[12] Anderson G K, Snyder H and Coogan J 1999 *Plasma Chem. Plasma Proc.* **19** 131–51

[13] Odic E, Paradisi M, Rea M, Parissi L, Goldman A and Goldman M 1999 Treatment of organic pollutants by corona discharge plasma *NATO ARW on Modern Problems of Electrostatics with Applications in Environment Protection (NATO ASI Series I)* ed I Inculet and R Cramarius (New York: Plenum) pp 143–60

[14] Ogata A, Shintani N, Mizuno K, Kushiyama S and Yamamoto T 1999 *IEEE Trans. Indust. Appl.* **35** 753–9

[15] Francke K P, Miessner H, Rudolph R and Rutkowski J 1998 Removal of VOCs by plasmocatalysis *11th Symp. on Elem. Proc. and Chem. Reactions in Low Temp. Plasma (Low Tatras, Slovakia)* ed M Morvová and K Hensel Contrib. Papers 1, pp 63–4

[16] Lesueur H, Czernichowski A and Chapelle J 1994 *Int. J. Hydrogen Energy* **19** 139–44

[17] Chelouah A, Marode E, Hartmann G and Achat S 1994 *J. Phys. D: Appl. Phys.* **27** 940–5

[18] Chang J S, Kohno H, He W, BerezinA A, Looy P C, Iijima K, Honda S, Matsumoto S and Shibuya A 1993 Dissociation of methane by atmospheric glow discharges in a capillary tube plasma reactor *Int. Symp. on High Pressure Low Temperature Plasma Chemistry, HAKONE IV (Bratislava, Slovakia, August–September 1993)* pp 171–6

[19] Akishev Yu S, Napartovich A P and Trushkin N I 1996 Decomposition of VOC at ppm levels using DC glow discharge plasmas *Int. Symp. on High Pressure Low Temperature Plasma Chemistry, HAKONE V (Mílovy, Czech Republic, September 1996)* pp 123–4

[20] Kohno H, Berezin A, Chang J S, Tamura M, Yamamoto T, Shibuya A and Honda S 1998 *IEEE Trans. Indust. Appl.* **34** 953–66

[21] Browning E 1965 *Toxicity and Metabolism of Industrial Solvents* (Amsterdam: Elsevier)

[22] Machala Z, Morvová M and Marode E 1998 Removal of cyclohexanone using high pressure pulseless glow discharge *Int. Symp. on High Pressure Low Temperature Plasma Chemistry, HAKONE VI (Cork, Ireland, August–September 1998)* pp 250–4

[23] Futamura S, Zhang A and Einaga H 1998 Involvement of active oxygen species in plasma chemical decomposition of volatile hydrocarbons *The Asia–Pacific Workshop on*

Water and Air Treatment by Advanced Techn.: Innovation and Commercial Appl. (December 1998) pp 87–90
[24] Bailey A, Stanley A W and Williams M R 1992 Gas phase decomposition of organic vapours in dc corona discharges *10th Int. Conf. on Gas Discharges and Their Application, (Swansea 1992)* pp 356–9
[25] Morvová M 1998 *J. Phys. D: Appl. Phys.* **31** 1865–74
[26] Morvová M, Hanic F and Morva I 2000 *J. Thermal Anal. Calorimetry* **61** 273–87
[27] Hanic F, Morvová M and Morva I 2000 *J. Thermal Anal. Calorimetry* **60** 1111–21
[28] Machala Z, Morvová M, Marode E and Morva I 1998 Removal of aromatic VOCs using high pressure pulseless glow discharge *11th Symp. on Elementary Processes and Chemical Reactions in Low Temperature Plasma (Low Tatras, Slovakia, June 1998)* ed M Morvová and K Hensel Contrib. Papers 2, pp 227–31
[29] Machala Z, Marode E and Morvová M 1998 Study of the pulseless (d.c.) high pressure glow discharge *Int. Symp. on High Pressure Low Temperature Plasma Chemistry, HAKONE VI (Cork, Ireland, August–September 1998)* pp 303–7
[30] Marode E, Goldman A and Goldman M 1993 High pressure discharge as a trigger for pollution control *Non-Thermal Plasma Techniques for Pollution Control (Nato ASI series, Part B)* ed B M Penetrante and S E Schultheis (Berlin: Springer) pp 167–90
[31] Chelouah A, Marode E and Hartmann G 1994 *J. Phys. D: Appl. Phys.* **27** 770–80
[32] Tholl A 1970 *Z. Naturf.* **259** 420
[33] Marode E 1975 *J. Appl. Phys.* **46** 2005
[34] Gallimberti I 1979 Invited lecture *Proc. 9th Int. Conf. Phen. Ion. Gas (Grenoble, France), J. Physique* Supp **40** C7 193
[35] Marode E, Bastien F and Hartmann G 1986 *(NATO Series ASI, Series B, vol 149)* p 95
[36] Nicolls R W 1962 *J. Quant. Spectrosc. Radiat. Trans.* **2** 433
[37] Albugues F, Birot A, Blanc D, Brunet H, Galy J, Millet P and Millet P 1971 *J. Chem. Phys.* **61** 2695
[38] Calo J M and Axtmann R C 1971 *J. Chem. Phys.* **54** 1332
[39] Lofthus A and Krupenie P H 1977 *J. Phys. Chem. Ref. Data* **6** 113–307
[40] Zhubanov B A, Agashkin O V and Ruchina L B 1984 *Atlas of IR Spectra of Heterocyclic Monomers and Polymers* (Kazakhstan: Nauka Alma Ata)